Simulated photodetachment spectra of AlH$_2^-$

Daniel K. W. Mok, Edmond P. F. Lee, Foo-tim Chau, and John M. Dyke

View Online   **Export Citation**   **CrossMark**

ARTICLES YOU MAY BE INTERESTED IN

Effective method to compute Franck-Condon integrals for optical spectra of large molecules in solution
The Journal of Chemical Physics **126**, 084509 (2007); https://doi.org/10.1063/1.2437197

Photoelectron spectroscopy of the aluminum hydride anions: AlH$_2^-$, AlH$_3^-$, Al$_2$H$_6^-$, Al$_3$H$_9^-$, and Al$_4$H$_{12}^-$
The Journal of Chemical Physics **138**, 124303 (2013); https://doi.org/10.1063/1.4796200

Effective method for the computation of optical spectra of large molecules at finite temperature including the Duschinsky and Herzberg–Teller effect: The Q_x band of porphyrin as a case study
The Journal of Chemical Physics **128**, 224311 (2008); https://doi.org/10.1063/1.2929846

Simulated photodetachment spectra of AlH$_2^-$

Daniel K. W. Mok,[1,a)] Edmond P. F. Lee,[1,2,a)] Foo-tim Chau,[1] and John M. Dyke[2]
[1]*Department of Applied Biology and Chemical Technology, The Hong Kong Polytechnic University, Hung Hom, Hong Kong*
[2]*School of Chemistry, University of Southampton, Highfield, Southampton SO17 1BJ, United Kingdom*

We have carried out high-level *ab initio* calculations on AlH$_2$ and its anion, as well as Franck-Condon factor calculations, which include anharmonicity and Duschinsky rotation, to simulate the photodetachment spectrum of AlH$_2^-$, with the aim of assigning the very recently reported photodetachment spectrum of AlH$_2^-$ [X. Zhang, H. Wang, E. Collins, A. Lim, G. Ganteför, B. Kiran, H. Schnöckel, B. Eichhorn, and K. Bowen, J. Chem. Phys. **138**, 124303 (2013)]. However, our simulated spectra do not support the assignment of the reported experimental spectrum to AlH$_2^-$. © *2013 AIP Publishing LLC*. [http://dx.doi.org/10.1063/1.4811671]

Very recently, Bowen *et al.* published the photodetachment spectra of some aluminium hydride anions.[1] The first band of the smallest aluminium hydride anion, AlH$_2^-$, reported has an onset at an electron affinity (EA) value of ∼0.5 eV, and extends to a detachment energy of ∼2.5 eV. The vertical detachment energy (VDE) and adiabatic EA value extracted from this band are 1.5 ± 0.1 and 0.9 ± 0.1 eV, respectively. The EA value was estimated assuming that hot bands often account for the first ∼0.2 eV of observed intensity, and by comparison with previous computed density functional theory (DFT) results.[2] However, although the vibrational frequencies of AlH$_2$ are available computationally[3–10] and experimentally,[4,5,7,11,12] no vibrational assignment of the partially resolved vibrational structure in this band has been given in Ref. 1, presumably because the complexity of the observed vibrational structure precluded any simple or straightforward assignment. In this connection, we have carried out state-of-the-art *ab initio* calculations and anharmonic Franck-Condon factor (FCF) calculations,[13,14] in order to simulate the vibrational structure of the first photodetachment band of AlH$_2^-$, with the aim of assisting its vibrational assignment. This procedure has been used successfully to assign the photodetachment spectra of several triatomic negative ions.[14–18] However, as will be shown below, comparison between simulated and experimental spectra suggests that the experimental spectrum assigned to AlH$_2^-$ in Ref. 1 is unlikely to be due to AlH$_2^-$.

In the present work, B3LYP calculations were carried out using G09,[19] while RCCSD(T) and UCCSD(T)-F12x (x = a or b)[20] calculations were performed using MOLPRO[21] (see footnotes of Table I for details). Specifically, Al $2s^2 2p^6$ core electrons were explicitly correlated in both RCCSD(T) and UCCSD(T)-F12x calculations. Large (up to 5Z quality) and appropriate (core-valence) basis sets were employed, and extrapolation to the complete basis set limit (CBS) was carried out using the $1/X^3$ formula.[22] Computed EA values of AlH$_2$, as well as geometrical parameters and vibrational fre-

quencies, for AlH$_2^-$ and AlH$_2$ are summarized in Table I, together with previously published values. Summarizing, computed results obtained in the present study agree very well with available computed and experimental values. The best computed EA (or EA$_e$) and EA$_0$ {EA$_e$ + zero-point-energy correction (ΔZPE)} values of AlH$_2$ are 1.068 and 1.11 eV (Table I), which agree very well with that reported in a recent coupled-cluster study on some group IIIa hydrides (the best EA value obtained at the CBS limit for AlH$_2$ is 1.10 eV).[23]

For spectral simulation, 91 and 115 UCCSD(T)-F12b energy points for the $\tilde{X}^1A_1$ state of AlH$_2^-$ (1.45 ≤ r ≤ 3.0 Å, 70 ≤ θ ≤ 140°, energies up to ∼3.16 eV above the minimum) and the $\tilde{X}^2A_1$ state of AlH$_2$ (1.25 ≤ r ≤ 3.0 Å, 75 ≤ θ ≤ 155°, energies up to ∼4.24 eV above the minimum), respectively, were computed and fitted to potential energy functions (PEFs) of a polynomial form.[13,14] The root-mean-square deviations of the fittings are 2.3 and 5.2 cm^{-1}. Computed harmonic (ω) and fundamental (υ) vibrational frequencies, obtained from variational calculations, of the υ_1 (symmetric stretching) and υ_2 (bending) modes of the two electronic states studied are given in Table I. The harmonic basis sets used in the anharmonic vibrational wavefunction calculations for the two electronic states considered are $\langle v_1'' \leq 5, v_2'' \leq 10 \rangle$ and $\langle v_1' \leq 7, v_2' \leq 18 \rangle$. Employing larger harmonic basis sets gives negligible changes in the computed anharmonic vibrational energies (<1 cm^{-1}). FCFs including anharmonicity and Duschinsky rotations were then calculated.[13,14] We have also employed the ezSpectrum code[24] to compute the FCFs within the harmonic oscillator model. Some simulated spectra (computed FCFs fitted to a Gaussian line shape with a selected full-width-at-half maximum, FWHM) and/or computed FCFs obtained at various selected Boltzmann vibrational temperatures are shown in Figures 1–3. It can be seen from Figure 1 that the vibrational structures obtained from the two sets of FCFs at 0 K within the harmonic oscillator model using ezSpectrum (middle bar diagram) and including anharmonicity using our ANFCF code[13,14] (top trace) are quite similar. This similarity suggests that anharmonic effects on the computed FCFs are small, and also supports the reliability of the simulated vibrational envelopes. The effects of hot bands in

a)Authors to whom correspondence should be addressed. Electronic addresses: bcdaniel@polyu.edu.hk and epl@soton.ac.uk

TABLE I. Optimized geometrical parameters (r/θ in Å/degrees), computed harmonic (ω; a_1, a_1, b_2) and fundamental (υ; in square brackets) vibrational frequencies (in cm^{-1}) of the $\widetilde{X}^1A_1$ state of AlH_2^- and the $\widetilde{X}^2A_1$ state of AlH_2, and computed electron affinities (EA_e in eV).

Method	AlH_2^-		AlH_2		EA_e
	r, θ	ω	r, θ	ω	
B3LYP/6-311++G**	1.699,94.6	1472,809,1464	1.604,118.1	1813,770,1858	1.05
RCCSD(T)/AVQZ[a]	1.686,95.3	1513,803,1503	1.597,118.5	1857,769,1890	1.06
RCCSD(T)/AVCQZ[b]	1.678,95.1	1514,808,1502	1.588,118.4	1862,775,1896	1.06
RCCSD(T)/AVC5Z[c]	1.678,95.0		1.588,118.4		1.06
RCCSD(T)/CBS[d]	1.677,95.0		1.588,118.4		1.07
UCCSD(T)-F12a/AVCQZ[e]	1.678,95.1		1.588,118.2		1.08[f]
UCCSD(T)-F12b/AVCQZ[e]	1.677,95.2	1519,813,− [1471],[804],−	1.588,118.2	1864,771,− [1825],[778],−	1.07[g]
Previous works					
MRDCI/∼TZP[h]			1.61,118	1760,750,2240	
VWN-PW-P/TZP;DZP[i]			1.609,118.2	1761,751,1827	
CCSD(T,ET4)/TZP;DZP[i]			1.602,118.7	1865,775,1901	
CCSD(T,ET4)/TZP;D95++[i]			1.608,118.3	1812,760,1849	
MBPT2/DZP[j]			1.558,118.0	1946,712,1999	
RCCSD(T)/aug-cc-pVTZ[k]			1.601,118.7		
MRSDCI/6-31G(p,spd)[l]			1.60,119.0		
BPW91/6311G**[m]			1.62,118.1		0.90
B3LYP/6-311++G**,[n]	1.699,94.6	1474,809,1466	1.603,118.1	1817,769,1862	1.10
QCISD[o]			1.592,118.1	1881,781,1910	
Matrix IR[p]				1770–1795, 766–771, 1806–1825	

[a]Aug-cc-pVQZ for all species; Al $1s^22s^22p^6$ electrons frozen.
[b]Aug-cc-pwCVQZ and aug-cc-pVQZ for Al and H, respectively; Al $1s^2$ electrons frozen.
[c]Aug-cc-pwCV5Z and aug-cc-pV5Z for Al and H, respectively; Al $1s^2$ electrons frozen.
[d]Extrapolation to the CBS limit using the $1/X^3$ formula.
[e]The various basis sets used for Al (H) are as follows: AO: aug-cc-pwCVQZ (aug-cc-pVQZ); DF: aug-cc-pwCVQZ-MP2FIT (aug-cc-pVQZ-MP2FIT); DF (for Fock and exchange matrices): aug-cc-pVQZ-JKFIT (aug-cc-pVQZ-JKFIT); RI: cc-pCVQZ-F12_OPTRI (aug-cc-pVQZ-JKFIT). The scaled perturbative triples obtained by a simple scaling factor, $\Delta E(T_{sc}) = \Delta E(T) \times E_{corr}^{MP2-F12}/E_{corr}^{MP2}$ have been used throughout.
[f]Using computed UCCSD(T)-F12a energies; Al $1s^2$ electrons frozen.
[g]Using computed UCCSD(T)-F12b energies; Al $1s^2$ electrons frozen.
[h]Reference 3.
[i]Reference 4.
[j]Reference 5.
[k]Reference 9.
[l]Reference 10; UMP2/6-31G(p,spd) results are consistent with MRSDCI results (see references therein for earlier calculations).
[m]Reference 2.
[n]Reference 7; AlH_2^- is 25.3 kcal.mol^{-1} lower in energy than AlH_2.
[o]Reference 8.
[p]References 4, 5, 7, 11, and 12.

the simulated spectra obtained at various Boltzmann vibrational temperatures are shown in Figure 1 (0 and 1500 K) and 2 (2500 K). The experimental spectrum of Ref. 1 is given in Figure 2 for comparison. It can be seen from Figure 1 that the simulated vibrational structure consists of mainly two progressions in the symmetry bending (υ_2) and stretching (υ_1) modes. This is consistent with the computed geometry change of ∼23° in bond angle and ∼0.09 Å in bond length (see Table I) upon the AlH_2 ($\widetilde{X}^2A_1$) ← AlH_2^- ($\widetilde{X}^1A_1$) photodetachment. Although simulated hot bands at elevated vibrational temperatures (1500 and 2500 K) complicate the simulated spectra and increase the spectral intensity of the photodetachment band in the low EA region (Figures 1 and 2), the simulated vibrational structure in the bending mode (computed $\upsilon_2 = 778$ cm^{-1} and experimental values ∼770 cm^{-1}; see Table I) at the low photodetachment energy region is resolvable with an FWHM of 35 meV (∼280 cm^{-1}; the experimental resolution given in Ref. 1 at 1 eV electron kinetic energy). However, although the experimental spectrum

(Figure 2 top trace) has some partially resolved vibrational structure, the overall vibrational envelope is very different from those of the simulated spectra obtained at different vibrational temperatures. Summing up, it is not possible to obtain a reasonable match between simulated and experimental spectra. Therefore, it is concluded that spectral simulations do not support the assignment of the observed spectrum reported in Ref. 1 to be solely due to the AlH_2 ($\widetilde{X}^2A_1$) ← AlH_2^- ($\widetilde{X}^1A_1$) photodetachment, or even to this process at all.

The complex vibrational structure observed in the experimental photodetachment spectrum assigned to AlH_2^- in Ref. 1 does not appear to be due to a single photodetachment band of a triatomic molecular anion. In this connection, further calculations were carried out on low-lying excited states of AlH_2^-, in order to determine if photodetachment from some low-lying excited states of AlH_2^- may contribute to the low photodetachment energy region of the first photodetachment band of AlH_2^-. At the B3LYP/6-311++G** level, the $\widetilde{X}^1A_1$ state of AlH_2^- has the outermost electronic
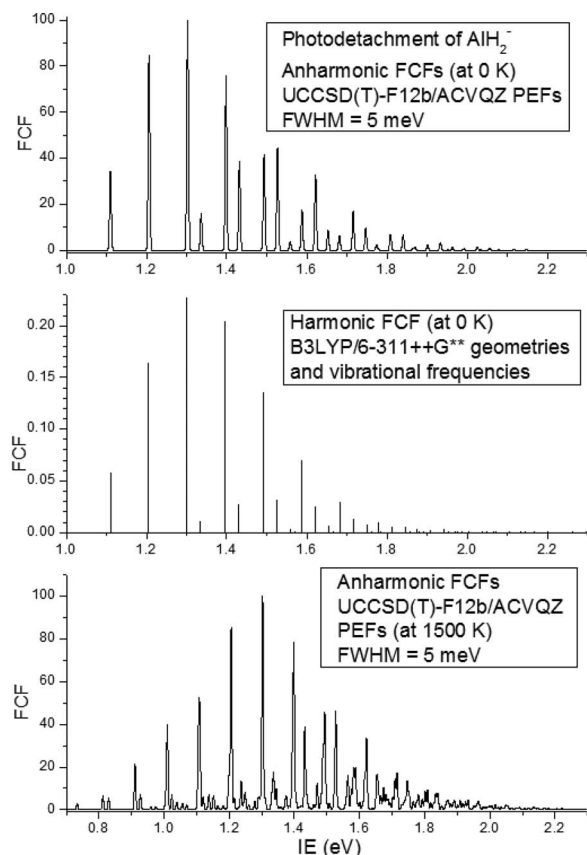
FIG. 1. Simulated photodetachment spectra (FWHM of 5 meV) from the $\tilde{X}^2A_1$ state of AlH_2^- to the $\tilde{X}^1A_1$ state of AlH_2 using computed anharmonic FCFs obtained with the UCCSD(T)-F12b/ACVQZ PEFs of the two states involved at the Boltzmann vibrational temperatures of 0 (top trace) and 1500 (bottom trace) K, and computed harmonic FCFs (middle bar diagram) using B3LYP/6-311+G** geometries and vibrational frequencies (at 0 K).
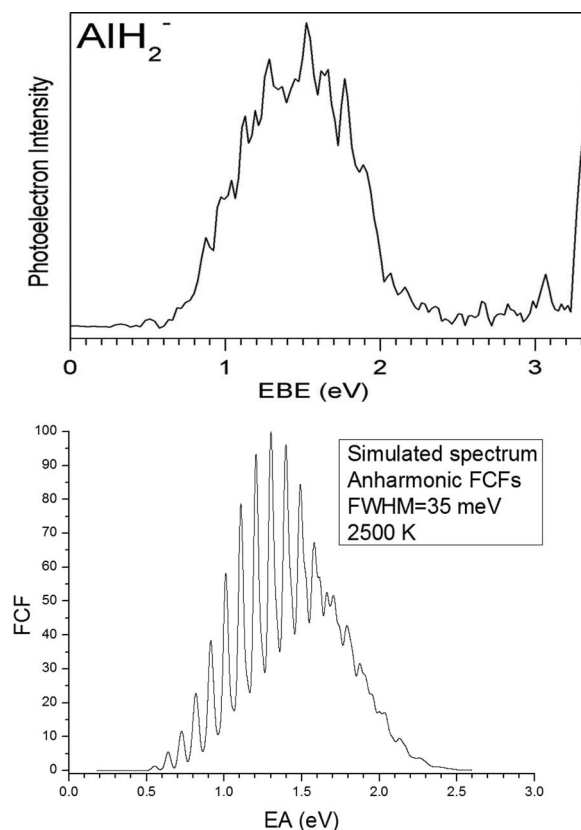

FIG. 2. Comparison between simulated (bottom trace; FWHM = 35 meV, at 2500 K) and experimental (top trace from Ref. 1) photodetachment spectra of AlH_2^-. Top trace reprinted with permission from X. Zhang *et al.*, J. Chem. Phys. **138**, 124303 (2013). Copyright 2013 AIP Publishing LLC.

configuration of $\ldots(1b_1)^2(5a_1)^2$ and the lowest-lying triplet state is a $^3B_1$ state with a $\ldots(5a_1)^1(2b_1)^1$ electronic configuration. At the TD-B3LYP/6-311++G** level, the first excited singlet state is a $^1B_1$ state (Table II). However, the $\tilde{A}^1B_1$ state has a computed negative EA value (-0.227 eV) to the $\tilde{X}^2A_1$ state of AlH_2 (Table II), and hence this state will not be further considered. For the $\tilde{a}^3B_1$ state, further calculations were performed at the RCCSD(T)/ACVQZ and UCCSD(T)-F12b/ACVQZ levels, and the results are given in Table II. FCF calculations for the AlH_2 ($\tilde{X}^2A_1$) ← AlH_2^- ($\tilde{a}^3B_1$) photodetachment were carried out within the harmonic oscillator model, and the computed harmonic FCFs together with those of the AlH_2 ($\tilde{X}^2A_1$) ← AlH_2^- ($\tilde{X}^1A_1$) photodetachment are shown in Figure 3 (top bar diagrams). The AlH_2 ($\tilde{X}^2A_1$) ← AlH_2^- ($\tilde{a}^3B_1$) photodetachment has a very strong adiabatic vibrational component, and very weak stretching and bending progressions, consistent with the very small computed geometry change upon photodetachment (Tables I and II). Comparing the experimental spectrum in Figure 2 (top trace) with the computed FCFs in Figure 3 (top bar diagrams), it is clear that including the AlH_2 ($\tilde{X}^2A_1$) ← AlH_2^- ($\tilde{a}^3B_1$) photodetachment does not help to match the simulated spectra to the observed spectrum assigned to AlH_2^- in Ref. 1.

In our recent work on the simulation of the photodetachment spectrum of CCl_2^-,[25] it was found that only part of the experimental photodetachment spectrum[26] could be assigned to CCl_2^-. Subsequently, it was found that the earlier experimental spectrum of Ref. 26 contained contributions from both CCl_2^- and $CHCl_2^-$, because the mass resolution of the mass analyser used in the experiment did not allow complete separation of CCl_2^- and $CHCl_2^-$.[27] We have, therefore, also considered the AlH_3 ($\tilde{X}^1A_1'$) ← AlH_3^- ($\tilde{X}^2A_1$) photodetachment in the present investigation, in case the experimental photodetachment band assigned to AlH_2^- may contain contributions from the AlH_3 ($\tilde{X}^1A_1'$) ← AlH_3^- ($\tilde{X}^2A_1$) band. Computed B3LYP/6-311++G** results on AlH_3 and its anion are summarized in Table II. Computed FCFs obtained within the harmonic oscillator model are shown in Figure 3 (bottom bar diagram). The vibrational structure of the AlH_3 ($\tilde{X}^1A_1'$) ← AlH_3^- ($\tilde{X}^2A_1$) photodetachment is very simple with a very strong adiabatic vibrational component and some weak vibrational components, namely $\{v_1'(a_1')\} = 1$ (AlH symmetric stretching mode) at 0.676 eV and $\{v_1' = 1, v_2'(a_2'') = 1\}$ (a_2'' umbrella mode in D_{3h} symmetry of AlH_3 and a_1 in C_{3v} symmetry of AlH_3^-; see Table II) at 0.765 eV. Interestingly, the vibrational envelope of the AlH_3 ($\tilde{X}^1A_1'$) ← AlH_3^- ($\tilde{X}^2A_1$) band based on the computed FCFs is very similar to that of the first band observed in the photoelectron spectrum of CH_3,[28] though the vibrational assignments are different {similar B3LYP and harmonic FCF calculations on CH_3/CH_3^+ were carried out and gave a very strong adiabatic vibrational component and a weak vibrational

TABLE II. Computed results (r, θ, ω, and EA in Å, degrees, cm^{-1}, and eV) of the lowest-lying triplet and singlet excited states of AlH$_2^-$, and the ground electronic states of AlH$_3^-$ and AlH$_3$.

AlH$_2^-$	$\widetilde{a}^3B_1$	$\widetilde{A}^1B_1$
	B3LYP/6-311++G**	**TD-B3LYP/6-311++G****
r/θ	1.625/118.9	1.616/122.1
ω(a$_1$,a$_1$,b$_2$)	1705, 722, 1736	1720, 677, 1776
EA	0.406	−0.227
	RCCSD(T)/ACVQZ	
r/θ	1.6119/117.98	
EA	0.451	
	UCCSD(T)-F12b/ACVQZ	
r/θ	1.6116/117.90	
EA	0.458	
	B3LYP/6-311++G**	
	AlH$_3^-$ (C$_{3v}$; ^{2}A$_1$)	**AlH$_3$** (D$_{3h}$; ^{1}A$_1'$)
r/θ(HAlH)	1.632/112.6	1.584/120.0
ω	582(a$_1$), 761(e), 1698(e),	713(a$_2''$), 799(e'), 1939(a$_1'$),
EA (EA$_0$)	1712(a$_1$)	1949(e') 0.378 (0.437)

progression of double quanta in the v_2'(a$_2''$) umbrella mode of CH$_3^+$ in agreement with the assignment given in the experimental study[28]}. The similarity in the vibrational envelopes between the AlH$_3$ ($\widetilde{X}^1A_1'$) ← AlH$_3^-$ ($\widetilde{X}^2A_1$) photodetachment and the CH$_3^+$ ($\widetilde{X}^1A_1'$) ← CH$_3$ ($\widetilde{X}^2A_1$) photoionization

FIG. 3. Computed harmonic FCFs of the AlH$_2$ ($\widetilde{X}^2A_1$) ← AlH$_2^-$ ($\widetilde{a}^3B_1$) and AlH$_2$ ($\widetilde{X}^2A_1$) ← AlH$_2^-$ ($\widetilde{X}^1A_1$) photodetachments at 0 K (top bar diagrams), and the AlH$_3$ ($\widetilde{X}^1A_1'$) ← AlH$_3^-$ ($\widetilde{X}^2A_1$) photodetachment at 0 K (bottom bar diagram; inserted the experimental spectrum assigned to AlH$_3^-$ from Ref. 1). Inset reprinted with permission from X. Zhang *et al.*, J. Chem. Phys. **138**, 124303 (2013). Copyright 2013 AIP Publishing LLC.

is because CH$_3$ (CH$_3^+$) are valence isoelectronic with AlH$_3^-$ (AlH$_3$), and the corresponding potential energy surfaces are also similar (both ionizations are from a very flat C$_{3v}$ structure to a D$_{3h}$ structure). In any case, computed FCFs of the AlH$_3$ ($\widetilde{X}^1A_1'$) ← AlH$_3^-$ ($\widetilde{X}^2A_1$) photodetachment band obtained here raise another issue: the assignment of the experimental photodetachment spectrum to AlH$_3^-$ in Ref. 1 is doubtful, as it is unlikely that the photodetachment band of AlH$_3^-$ would have such a complex vibrational structure as shown in the experimental spectrum assigned to AlH$_3^-$ in Ref. 1 {see inset (a) in Figure 3 bottom half}.

Summarizing, we have carried out state-of-the-art *ab initio* calculations on AlH$_2$ and AlH$_2^-$. Using computed UCCSD(T)-F12b/AVQZ PEFs, anharmonic FCFs including Duschinsky rotation were computed. Simulated photodetachment spectra, which include hot bands obtained at various vibrational temperatures, were compared with the experimental spectrum assigned to AlH$_2^-$ in Ref. 1. It is concluded that the observed spectrum cannot be due to AlH$_2^-$. In addition, photodetachment from low-lying excited states of AlH$_2^-$ and also possible contamination of the photodetachment spectrum assigned to AlH$_2^-$ by AlH$_3^-$ were considered, but both considerations could not resolve the discrepancies between the simulated spectra obtained in this work and the observed spectra assigned to AlH$_2^-$ and AlH$_3^-$ in Ref. 1. In conclusion, the assignments of the experimental photodetachment spectra of AlH$_2^-$ and AlH$_3^-$ in Ref. 1 are doubtful. Further investigations are required to establish the molecular anions associated with the observed spectra reported in Ref. 1, and to record the photodetachment spectra of AlH$_2^-$ and AlH$_3^-$.
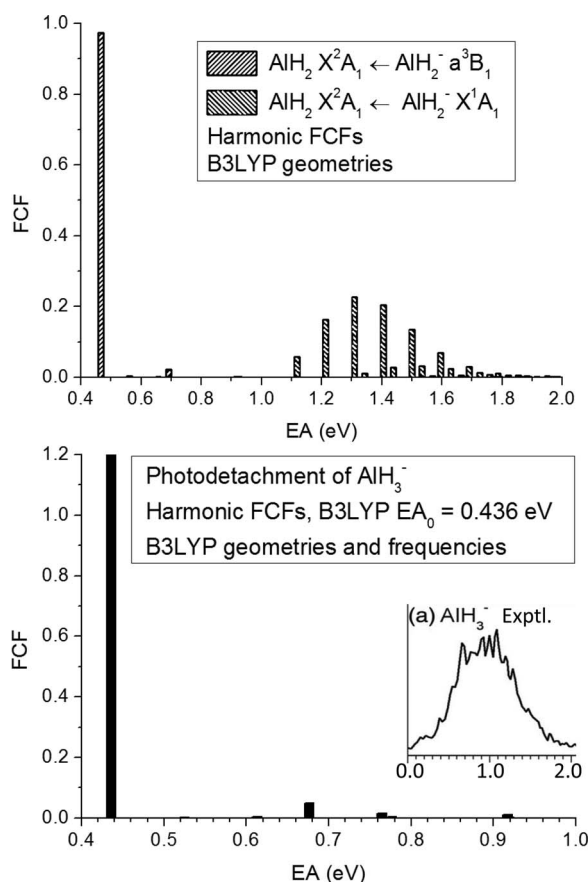
[1]X. Zhang, H. Wang, E. Collins, A. Lim, G. Ganteför, B. Kiran, H. Schnöckel, B. Eichhorn, and K. Bowen, J. Chem. Phys. **138**, 124303 (2013).

[2]B. K. Rao, P. Jena, S. Burkart, G. Ganteför, and G. Seifert, Phys. Rev. Lett. **86**, 692 (2001).

[3]B. Nestmann and M. Peric, Chem. Phys. **89**, 257 (1984).

[4]G. V. Chertihin and L. Andrews, J. Phys. Chem. **97**, 10295 (1993).

[5]P. Pullumbi, C. Mijoule, L. Manceron, and Y. Bouteiller, Chem. Phys. **185**, 13 (1994).

[6]M. T. Swihart and L. Catoire, Combust. Flame **121**, 210 (2000).

[7]X. Wang, L. Andrews, S. Tam, M. E. DeRose, and M. Fajardo, J. Am. Chem. Soc. **125**, 9218 (2003).

[8]J.-F. Sun, J.-M. Wang, D.-H. Shi, and J.-C. Zhang, Acta Phys. Sin. **55**, 4490 (2006).

[9]H. Partridge, C. W. Bauschlicher, Jr., and L. Visscher, Chem. Phys. Lett. **246**, 33 (1995).

[10]W.-H. Fang, Chem. Phys. Lett. **260**, 565 (1996).

[11]L. Andrews and X. Wang, J. Phys. Chem. A **108**, 4202 (2004).

[12]*NIST Chemistry WebBook*, NIST Standard Reference Database Number 69, edited by P. J. Linstrom and W. G. Mallard (National Institute of Standards and Technology, Gaithersburg, MD, 2011), see http://webbook.nist.gov.

[13]D. K. W. Mok, E. P. F. Lee, F.-T. Chau, D. C. Wang, and J. M. Dyke, J. Chem. Phys. **113**, 5791 (2000).

[14]F.-T. Chau, D. K. W. Mok, E. P. F. Lee, and J. M. Dyke, ChemPhysChem **6**, 2037 (2005).

[15]E. P. F. Lee, J. M. Dyke, D. K. W. Mok, and F.-t. Chau, J. Phys. Chem. A **112**, 4511 (2008).

[16]D. K. W. Mok, F.-t. Chau, J. M. Dyke, and E. P. F. Lee, Chem. Phys. Lett. **458**, 11 (2008).

[17]E. P. F. Lee, D. K. W. Mok, F.-T. Chau, and J. M. Dyke, J. Comput. Chem. **30**, 337 (2009).

[18]D. K. W. Mok, E. P. F. Lee, F.-T. Chau, and J. M. Dyke, Phys. Chem. Chem. Phys. **10**, 7270 (2008).

[19]M. J. Frisch, G. W. Trucks, H. B. Schlegel *et al.*, GAUSSIAN 09, Revision C.1, Gaussian, Inc., Wallingford, CT, 2009.

[20]G. Knizia, T. B. Adler, and H.-J. Werner, J. Chem. Phys. **130**, 054104 (2009).

[21]H.-J. Werner, P. J. Knowles, R. Lindh, F. R. Manby, M. Schütz *et al.*, MOLPRO, version 2009.1, a package of *ab initio* programs, 2009, see http://www.molpro.net.

[22]A. Halkier, T. Helgaker, W. Klopper, P. Jorgensen, and A. G. Csaszar, Chem. Phys. Lett. **310**, 385 (1999).

[23]I. Černušáka, A. Zavažanováa, J. Raaba, and P. Neográdya, Collect. Czech. Chem. Commun. **68**, 75 (2003).

[24]See http://iopenshell.usc.edu/ downloads for V. A. Mozhayskiy and A. I. Krylov, ezSpectrum; this work was conducted using the resources of the iOpenShell Center for Computational Studies of Electronic Structure and Spectroscopy of Open-Shell and Electronically Excited Species (http://iopenshell.usc.edu) supported by the National Science Foundation through the CRIF:CRF program.

[25]J. M. Dyke, E. P. F. Lee, D. K. W. Mok, and F. T. Chau, ChemPhysChem **6**, 2046 (2005).

[26]R. L. Schwartz, G. E. Davico, T. M. Ramond, and W. C. Lineberger, J. Phys. Chem. A **103**, 8213 (1999).

[27]S. W. Wren, K. M. Vogelhuber, K. M. Ervin, and W. C. Lineberger, Phys. Chem. Chem. Phys. **11**, 4745 (2009).

[28]J. M. Dyke, N. Jonathan, E. P. F. Lee, and A. Morris, J. Chem. Soc., Faraday Trans. 2 **72**, 1385 (1976).